Paper 209

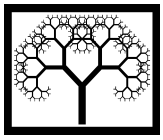

Proceedings of the Eleventh International Conference
on Computational Structures Technology,
B.H.V. Topping, (Editor),
Civil-Comp Press, Stirlingshire, Scotland

Two Scale Modelling of Acoustic Waves in Phononic Plates using Homogenization of High-Contrast Media

E. Rohan[1], R. Cimrman[2] and B. Miara[3]
[1] Department of Mechanics, Faculty of Applied Sciences
[2] New Technologies Research Centre
University of West Bohemia, Pilsen, Czech Republic
[3] Université Paris-Est, ESIEE, Noisy-le-Grand, France

Abstract

This paper deals with modeling wave dispersion in periodically heterogeneous plates characterised by high contrasts in elastic coefficients. We study two plate models based on the Reissner-Mindlin (R-M) theory and on the Kirchhoff-Love (K-L) theory. Models of homogenized plates were obtained using the two-scale unfolding method with the high contrast ansatz respected by scaling the elasticity coefficients of compliant inclusions. Consequently, dispersion properties are retained in the limit when the scale of the microstructure tends to zero. For some wavelengths, "mass density" coefficients can be negative, so that intervals of frequencies exist for which there is no propagation of elastic waves, the so-called band-gaps. Dispersion analysis for guided waves is performed for both types of the plates; occurrence of band gaps for the R-M plates is confirmed using numerical examples, however, the homogenized K-L plate model does not admit band gaps.

Keywords: phononic materials, plate models, homogenization, band gaps, wave dispersion.

1 Introduction

We consider problems of wave propagation in periodically heterogeneous plates with high contrasts in elastic coefficients. Following the approach of [1] and [7] we apply the unfolding method of homogenization [4] to obtain limit plate models. Two cases are studied: 1) according to the Reissner-Mindlin theory the plate deformation is described by the mid-plane deflections and by rotations of the plate cross-sections which account for the shear stress effects; 2) using the Kirchhoff-Love theory, the plate deflections are described by the bi-harmonic operator, thus neglecting the shear effects. In both cases we assume such heterogeneities which depend on the mid-plate

coordinates only, but do not change with the transversal coordinate. As an example we can consider plates with soft cylindrical inclusions. Under such restrictions the homogenization is applied to the plate equations with the elastic coefficients defined as periodically fluctuating functions associated with the heterogeneities. Due to the high contrast ansatz in scaling the elasticity coefficients of inclusions, as employed in [1, 6, 2, 3], dispersion properties are retained in the limit when the scale (the characteristic size) of the microstructure tends to zero.

Namely for the Reissner-Mindlin plates we show that, when the size of the microstructures tends to zero, the limit homogeneous structure presents the phononic effect: for some wavelengths, the mass coefficients associated with the inertia can be negative [6]. This means that there exist intervals of frequencies in which there is no propagation of elastic waves, the so-called band-gaps.

2 Heterogeneous plates

We consider heterogeneous structures associated with a given scale, say $\varepsilon_0 > 0$, which is the ratio between the characteristic lengths of the microscopic and the macroscopic description. There exist convergent sequences of solutions of the plate problems characterized by scales $\varepsilon \to 0$. For any fixed $\varepsilon > 0$ we shall rely on the following essential material properties.

The fourth order, bi-dimensional elasticity tensor $\mathbb{C} = (C^{ijkl})$ is symmetric $C_{ijkl} = C_{klij} = C_{ikjl}$ and positive definite. In particular, for the sake of simplicity, we consider isotropic materials only, which are characterized by two Lamé parameters. The plate model according the Reissner-Mindlin theory involves also the shear modulus, here treated formally as an independent parameter $\gamma > 0$, although it is associated with one of the Lamé parameters. The mass density ρ is positive.

We treat periodic composite materials, so that the material coefficients $\mathbb{C}$, γ and ρ are periodically oscillating functions in $\mathbb{R}^2$; it will be described in detail in Section 3.1

2.1 The Reissner–Mindlin plate model

The plate model can be derived by an asymptotic analysis of the elasticity problem imposed in $\Omega\times]-h,h[$, where $\Omega \subset \mathbb{R}^2$ is an open bounded domain with regular boundary $\partial\Omega$ and h is the plate thickness. In the time interval $[0,T]$ the plate undergoes the following two modes of displacements: the in-plane "membrane modes" described by $\boldsymbol{U} = (U_1, U_2) : [0,T] \times \bar{\Omega} \longrightarrow \mathbb{R}^2$, and the "off-plane" transversal deflections $W : [0,T] \times \bar{\Omega} \longrightarrow \mathbb{R}$; moreover the cross-sections undergo rotations $\boldsymbol{\Theta} = (\Theta_1, \Theta_2) : [0,T] \times \bar{\Omega} \longrightarrow \mathbb{R}^2$.

The displacement and rotation $(\boldsymbol{U}, W, \boldsymbol{\Theta})$ of the plate satisfy the equilibrium equa-

tions

$$\begin{cases} h\rho\dfrac{\mathrm{d}^2}{\mathrm{d}t^2}\boldsymbol{U} - h\mathrm{div}\boldsymbol{\sigma}(\boldsymbol{U}) = \boldsymbol{T} \quad \text{in } \Omega\,, \\ h\rho\dfrac{\mathrm{d}^2}{\mathrm{d}t^2}W - h\mathrm{div}\boldsymbol{\tau}(W,\boldsymbol{\Theta}) = F \quad \text{in } \Omega, \\ \dfrac{h^3}{3}\rho\dfrac{\mathrm{d}^2}{\mathrm{d}t^2}\boldsymbol{\Theta} - \dfrac{h^3}{3}\mathrm{div}\boldsymbol{\sigma}(\boldsymbol{\Theta}) - h\boldsymbol{\tau}(W,\boldsymbol{\Theta}) = \boldsymbol{M} \quad \text{in } \Omega, \\ \boldsymbol{U} = \boldsymbol{0}\,, \quad W = 0\,, \quad \boldsymbol{\Theta} = \boldsymbol{0} \quad \text{on } \partial\Omega\,. \end{cases} \tag{1}$$

with $\boldsymbol{\tau}$ and $\boldsymbol{\sigma}$ expressed by the following linear constitutive laws:

$$\begin{cases} \boldsymbol{\tau}(W,\boldsymbol{\Theta}) & := & \gamma(\nabla W - \boldsymbol{\Theta}), & \text{shear stress due to relative (to mid-plane) rotation of cross-s.} \\ \boldsymbol{\sigma}(\boldsymbol{\Theta}) & := & \mathbb{C}\boldsymbol{e}(\boldsymbol{\Theta})\,, & \text{normal stress due to bending induced by rotations} \\ \boldsymbol{\sigma}(\boldsymbol{U}) & := & \mathbb{C}\boldsymbol{e}(\boldsymbol{U})\,, & \text{normal stress due to the in-plane membrane modes.} \end{cases} \tag{2}$$

In general, we may consider a general decomposition of $\partial\Omega$ with respect to the above displacements and rotations into the "Neumann" and "Dirichlet" parts of the boundary. However, for the sake of simplicity, we consider the fully supported and clamped plate.

The linearized deformation tensor $e(\boldsymbol{\Theta}) = (e_{ij}(\boldsymbol{\Theta}))$ is given by the symmetric gradient $\boldsymbol{e}(\boldsymbol{\Theta}) = 1/2\,(\partial_j\Theta_i + \partial_i\Theta_j)$, $i,j = 1,2$.

We shall consider solutions in the form of harmonic stationary waves induced by harmonic loading

$$\boldsymbol{T}(x,t) = \boldsymbol{t}(x)\exp\{\mathrm{i}\omega t\}\,, \qquad F(x,t) = f(x)\exp\{\mathrm{i}\omega t\}\,, \qquad \boldsymbol{M}(x,t) = \boldsymbol{m}(x)\exp\{\mathrm{i}\omega t\}\,, \tag{3}$$

where ω is a given frequency, so that

$$\boldsymbol{U}(x,t) = \boldsymbol{u}(x)\exp\{\mathrm{i}\omega t\}\,, \qquad W(x,t) = w(x)\exp\{\mathrm{i}\omega t\}\,, \qquad \boldsymbol{\Theta}(x,t) = \boldsymbol{\theta}(x)\exp\{\mathrm{i}\omega t\}\,. \tag{4}$$

On substituting (3) into (1), we get the following equations governing the amplitudes $(\boldsymbol{u}, w, \boldsymbol{\theta})$:

$$\begin{cases} -\omega^2 h\rho\boldsymbol{u} - h\mathrm{div}\boldsymbol{\sigma}(\boldsymbol{u}) = \boldsymbol{t} \quad \text{in } \Omega\,, \\ -\omega^2 h\rho w - h\mathrm{div}\boldsymbol{\tau}(w,\boldsymbol{\theta}) = f \quad \text{in } \Omega, \\ -\omega^2\dfrac{h^3}{3}\rho\boldsymbol{\theta} - \dfrac{h^3}{3}\mathrm{div}\boldsymbol{\sigma}(\boldsymbol{\theta}) - h\boldsymbol{\tau}(w,\boldsymbol{\theta}) = \boldsymbol{m} \quad \text{in } \Omega, \\ \boldsymbol{u} = 0, \quad w = 0, \quad \boldsymbol{\theta} = 0 \quad \text{on } \partial\Omega. \end{cases} \tag{5}$$

2.2 The Kirchhoff–Love plate model

The motion of the plate is given by the out-off plate deflections W and by the in-plane (membrane modes) displacements $\boldsymbol{U}$. Let us recall that this kind of plate does not admit any relative rotation of the plate cross-sections w.r.t. the plate mean surface, therefore, it is convenient rather for thin plates.

We shall consider solutions in the form of harmonic stationary waves induced by harmonic loading, see (3). Thus, in analogy with (4), for a given fixed frequency ω, the amplitudes $(\boldsymbol{u}, w)$ satisfy

$$\begin{cases} -\omega^2 h\rho\boldsymbol{u} - h\mathrm{div}\boldsymbol{\sigma}(\boldsymbol{u}) = \boldsymbol{t} \quad \text{in } \Omega\,, \\ \dfrac{h^3}{3}\nabla\nabla : \boldsymbol{\Sigma}(w) - \omega^2\rho\left(hw - \dfrac{h^3}{3}\nabla\cdot\nabla w\right) = f - \nabla\cdot\boldsymbol{m} \quad \text{in } \Omega\,, \\ w = 0, \quad \boldsymbol{n}\cdot\nabla w = 0, \quad \boldsymbol{u} = 0 \quad \text{on } \partial\Omega\,, \end{cases} \tag{6}$$

where $\nabla\nabla v = (\partial^2 v/\partial x_i \partial x_j)$ is the 2nd order differential operator and stresses $\boldsymbol{\sigma}$ and $\boldsymbol{\Sigma}$ are given in terms of the elasticity tensor, as follows:

$$\begin{aligned} \boldsymbol{\sigma}(\boldsymbol{u}) &= \mathbb{C}\boldsymbol{e}(\boldsymbol{u})\,, \\ \boldsymbol{\Sigma}(w) &= \mathbb{C}\nabla\nabla w = \boldsymbol{\sigma}(\nabla w)\,. \end{aligned} \tag{7}$$

3 Homogenization

We consider a plate made of a heterogeneous material, whereby its periodic structure is defined in the reduced $2D$ configuration directly. As usual, we use small parameter ε describing the characteristic size of the microstructure. The solutions of (5) and (6) depend upon ε, which will be indicated by the superscript $\square^\varepsilon$. Using asymptotic analysis, the limit model for $\varepsilon \to 0$ can be obtained which describes behaviour of the homogenized material. Details on the homogenization procedure are out of the scope in this short paper, interested readers are referred to associated publications [4] and [1, 6].

Remark on the "in-plane" membrane modes. In the rest of the paper we consider just the out-of-plane "deflection" and "rotation" modes of plate deformation, since, in the linear theory used here, there is no coupling between these modes and the "membrane" modes described by displacements $\boldsymbol{u}$. The "membrane" modes satisfying $(1)_1$ and $(5)_1$ are driven by the same type of equations as in the 3D elasticity which was discussed in papers [1, 7, 2, 3].

3.1 Strongly heterogeneous periodic composite

We assume the plate Ω is constituted by the matrix Ω_m^ε and by periodically distributed inclusions; their collection forms domain Ω_c^ε. The split of Ω is subject to the following constraints.

1. $\Omega_m^\varepsilon, \Omega_c^\varepsilon \subset \Omega \subset \mathbb{R}^2$ and $\Omega_m^\varepsilon \cap \Omega_c^\varepsilon = \emptyset$,
2. $\Omega = \Omega_m^\varepsilon \cup \Omega_c^\varepsilon \cup \Gamma^\varepsilon$, where $\Gamma^\varepsilon = \overline{\Omega_m^\varepsilon} \cap \overline{\Omega_c^\varepsilon}$.
3. matrix: Ω_m^ε is connected. As the result, inclusions Ω_c^ε are disconnected.

The microstructure is generated as a periodic lattice using the representative periodic cell (RPC) denoted by Y. For simplicity, we consider a rectangular RPC with the following definition: $Y = \Pi_{i=1}^{2}]0, \bar{y}_i[\subset \mathbb{R}^2$ ($\mathbb{R}$ being the set of real numbers) where $\bar{y}_i > 0$ can be chosen so that $|Y| = 1$. The RPC is decomposed in accordance with Ω, i.e. $Y_m \subset Y$ and $Y_c = Y \setminus \overline{Y_m}$ are strictly contained in Y.

The coordinates of any point in Ω can be split into a "coarse" part $\xi = (\xi_i)$ and a "fine" part $y = (y_i)$, also called fast and slow evolving parts: For a given finite $\varepsilon > 0$ we have the unique decomposition

$$\begin{aligned} x &\equiv \varepsilon \left[\frac{x}{\varepsilon}\right]_Y + \varepsilon \left\{\frac{x}{\varepsilon}\right\}_Y \\ &= \xi + \varepsilon y \ , \ \text{ where } y = \left\{\frac{x}{\varepsilon}\right\}_Y \in Y \ \text{ and } \xi = \varepsilon \left[\frac{x}{\varepsilon}\right]_Y \in \Omega \ , \end{aligned} \tag{8}$$

where $\xi_i = \varepsilon k_i \bar{y}_i$, $i = 1, 2$, $k_i \in \mathbb{Z}$ is the lattice coordinate. Such a decomposition is unique, once $Y \in \mathbb{R}^2$ is defined. Note that $[z_i/\bar{y}_i]_Y$ (no summation) is the integer part of $z_i/\bar{y}_i$ and $\{z_i/\bar{y}_i\}_Y$ is the remainder. We shall consider $\bar{y}_i = 1$, $i = 1, 2$.

Material parameters $\mathbb{C}^\varepsilon = (C^\varepsilon_{ijkl})$ and γ^ε are periodically oscillating. For the sake of simplicity we shall consider only piecewise constant material. To retain the phononic effect in the homogenized plate, following the analogous approach employed in the case of phononic 3D periodic structures, we introduce the scaling of the material coefficients in the inclusions:

$$\begin{aligned} \mathbb{C}^\varepsilon(x) &= \chi^\varepsilon_c(x)\varepsilon^2 \mathbb{C}^c + \chi^\varepsilon_m(x)\mathbb{C}^m \ , \\ \gamma^\varepsilon(x) &= \chi^\varepsilon_c(x)\varepsilon^2 \gamma^c + \chi^\varepsilon_m(x)\gamma^m \ . \end{aligned} \tag{9}$$

We recall the standard properties of constant tensors $\mathbb{C}^c, \mathbb{C}^m$ and coefficients γ^c, γ^m which usually are considered: there exist constants $0 < \underline{m} < \overline{m} < \infty$ independent of ε such that (recall $|\boldsymbol{e}|^2 = e_{ij}e_{ij}$),

$$\begin{aligned} &C^m_{ijkl} e_{ij} e_{kl} \geq \underline{m} |\boldsymbol{e}|^2 \quad \forall \boldsymbol{e} = (e_{ij}) \in \mathbb{R}^{2\times 2}, \quad e_{ij} = e_{ji} \ , \quad \sup_{x\in\Omega} |C^m_{ijkl}| \leq \overline{m} \ , \\ &\underline{m} \leq \gamma^m \leq \overline{m} \ , \end{aligned} \tag{10}$$

and in analogy for $\mathbb{C}^c$ and γ^c. The rotation-deflection coupling coefficient $\gamma^\varepsilon(x)$, i.e. the shear stiffness, is only relevant for the Reissner-Mindlin plate model. It is worth noting that $\mathbb{C}^\varepsilon(x)$ and $\gamma^\varepsilon(x)$ are positive definite for $\varepsilon > 0$ only.

The density of the two materials is assumed to be of the same order of magnitude, therefore we shall consider

$$\begin{aligned} \rho^\varepsilon(x) &= \chi^\varepsilon_c(x)\rho^c + \chi^\varepsilon_m(x)\rho^m \ , \\ \underline{\rho} &\leq \rho^s \leq \overline{\rho} \ , \end{aligned} \tag{11}$$

where $\underline{\rho}, \overline{\rho}$ are given positive real numbers.

Some preliminaries The homogenized model was obtained using the periodic unfolding method which is based on the unfolding operator $\mathcal{T}_\varepsilon : v \in L^1(\Omega;\mathbb{R}) \to L^1(\Omega \times Y;\mathbb{R})$ defined, as follows, see [4],

$$\mathcal{T}_\varepsilon(v)(x,y) = \; v(\varepsilon \left[\tfrac{x}{\varepsilon}\right] + \varepsilon y) \; , \qquad x \in \Omega, y \in Y \; .$$

We shall use $H^1_\#(Y)$ and $H^2_\#(Y)$, the spaces of periodic (scalar) functions,

$$\begin{aligned} H^1_\#(Y) &= \{v \in H^1(Y) \mid v \text{ is Y-periodic } \} \; , \\ H^2_\#(Y) &= \{w \in H^2(Y) \mid w, \nabla_y w \;\; \text{are Y-periodic}\} \; , \end{aligned} \tag{12}$$

and the associated space of vector-valued functions $\mathbf{H}^1_\#(Y) = (H^1_\#(Y))^2$.

3.2 Reissner-Mindlin phononic plate

We apply the unfolding method of homogenization to obtain a limit model of the R-M plate for $\varepsilon \to 0$. The elastic standing waves are described by the solution of the following problem with the oscillating material coefficients: For a given frequency, find triplet $(w^\varepsilon, \boldsymbol{\theta}^\varepsilon) \in (H^1_0(\Omega))^3$ such that

$$\begin{aligned} &- h\omega^2 \int_\Omega \rho^\varepsilon \left(w^\varepsilon z^\varepsilon + \frac{h^2}{3} \boldsymbol{\theta}^\varepsilon \cdot \boldsymbol{\psi}^\varepsilon \right) \\ &+ h \int_\Omega [\gamma^\varepsilon(\nabla w^\varepsilon - \boldsymbol{\theta}^\varepsilon)] \cdot (\nabla z^\varepsilon - \boldsymbol{\psi}^\varepsilon) + \frac{h^3}{3} \int_\Omega [\mathbb{C}^\varepsilon e(\boldsymbol{\theta}^\varepsilon)] : e(\boldsymbol{\psi}^\varepsilon) \\ &= \int_\Omega (f z^\varepsilon + \boldsymbol{m} \cdot \boldsymbol{\psi}^\varepsilon) \; , \end{aligned} \tag{13}$$

for all $(z^\varepsilon, \boldsymbol{\psi}^\varepsilon) \in (H^1_0(\Omega))^3$.

Here we present the homogenized "macroscopic" model which involves homogenized coefficients describing the effective mass and elasticity coefficients. The standing waves propagating in the homogenized plate are described in terms of amplitudes $(\boldsymbol{\theta}, w) \in \mathbf{H}^1_0(\Omega) \times \in H^1_0(\Omega)$ which satisfy the following equations:

$$\begin{aligned} &- \omega^2 \int_\Omega \left(\frac{h^3}{3} [\boldsymbol{\mathcal{M}}(\omega^2)\boldsymbol{\theta}] \cdot \boldsymbol{\psi} + h\mathcal{N}(\omega^2) w z \right) \\ &+ \frac{h^3}{3} \int_\Omega [\boldsymbol{\mathcal{D}} \boldsymbol{e}_x(\boldsymbol{\theta})] : \boldsymbol{e}_x(\boldsymbol{\psi}) + h \int_\Omega [\boldsymbol{\mathcal{G}}(\nabla_x w - \boldsymbol{\theta})] \cdot (\nabla_x z - \boldsymbol{\psi}) \\ &= \int_\Omega \left([\boldsymbol{R}(\omega^2)\boldsymbol{m}] \cdot \boldsymbol{\psi} + S(\omega^2) f z \right) \quad \forall \boldsymbol{\psi} \in \mathbf{H}^1_0(\Omega), z \in H^1_0(\Omega) \; , \end{aligned} \tag{14}$$

where $\boldsymbol{\mathcal{D}}$ is the 4th order tensor of homogenized elasticity coefficients see (21), $\boldsymbol{\mathcal{G}}$ is the 2nd order tensor given in (22) describing the shear stiffness of the plate, $\boldsymbol{\mathcal{M}}(\omega^2)$ (the 2nd order tensor) and $\mathcal{N}(\omega^2)$ are homogenized mass coefficients. Below we explain how these coefficients are computed.

Characteristic microscopic responses. The homogenized coefficients are expressed in terms of the characteristic responses, the so-called corrector basis functions. We proceed in analogy with [1] where the 3D elasticity dynamic problems were considered. We employ the elasticity bilinear form

$$c_{Y_m}(\tilde{\boldsymbol{u}},\,\tilde{\boldsymbol{v}}) = \int_{Y_m} (\mathbb{C}^m \boldsymbol{e}_y(\tilde{\boldsymbol{u}})) : \boldsymbol{e}_y(\tilde{\boldsymbol{v}})\ . \tag{15}$$

The following characteristic responses depend exclusively on properties of the stiffer material in Y_m; two problems for the so-called corrector basis functions are to be solved:

- Find $\tilde{\boldsymbol{\theta}}^{rs} \in \mathbf{H}^1_{\#}(Y)/\mathbb{R}$ such that

$$c_{Y_m}\left(\tilde{\boldsymbol{\theta}}^{rs} + \boldsymbol{\Pi}^{rs},\,\tilde{\boldsymbol{v}}\right) = 0 \quad \forall \tilde{\boldsymbol{v}} \in \mathbf{H}^1_{\#}(Y_m)\ . \tag{16}$$

- Find $\tilde{w}^k \in H^1_{\#}(Y_m)/\mathbb{R}$ such that

$$\int_{Y_m} \gamma^m \nabla_y(\tilde{w}^k + y_k)\cdot\nabla_y\tilde{z} = 0 \quad \forall \tilde{z} \in H^1_{\#}(Y_m)\ . \tag{17}$$

To express the homogenized mass coefficients, we need the eigenfrequencies and eigenfunctions which describe vibration of the inclusions clamped into the matrix. Two eigenvalue problems with discrete spectra are solved:

- Find $(\boldsymbol{\Theta}^r, \lambda^r) \in \mathbf{H}^1_{\#0}(Y) \times \mathbb{R}$ for $r = 1, 2, \ldots$ such that (note $\boldsymbol{\Theta}^r = (\Theta^r_i)$)

$$\fint_{Y_c} [\mathbb{C}^c \boldsymbol{e}_y(\boldsymbol{\Theta}^r)] : \boldsymbol{e}_y(\boldsymbol{\psi}) = \lambda^r \fint_{Y_c} \rho \boldsymbol{\Theta}^r \cdot \boldsymbol{\psi} \quad \forall \boldsymbol{\psi} \in \mathbf{H}^1_{\#0}(Y)\ . \tag{18}$$

- Find $(W^r, \mu^r) \in H^1_{\#0}(Y_c) \times \mathbb{R}$ for $r = 1, 2, \ldots$ such that

$$\fint_{Y_c} [\gamma^c \nabla_y W^r]\cdot\nabla_y\zeta = \mu^r \fint_{Y_c} \rho W^r \zeta \quad \forall \zeta \in H^1_{\#0}(Y_c)\ . \tag{19}$$

The eigenfunctions are normalized, so that

$$\fint_{Y_c} \rho \boldsymbol{\Theta}^r \cdot \boldsymbol{\Theta}^s = \delta_{rs}\ , \qquad \fint_{Y_c} \rho W^r W^s = \delta_{rs}\ . \tag{20}$$

Homogenized coefficients. The homogenized plate elasticity is represented by the following two tensors:

- *Homogenized "in-plane" elasticity* $\mathcal{D} = (\mathcal{D}_{ijkl})$:

$$\begin{aligned} \mathcal{D}_{ijkl} &= c_{Y_m}\left(\tilde{\boldsymbol{\theta}}^{kl} + \boldsymbol{\Pi}^{kl},\,\boldsymbol{\Pi}^{ij}\right) \\ &= c_{Y_m}\left(\tilde{\boldsymbol{\theta}}^{kl} + \boldsymbol{\Pi}^{kl},\,\tilde{\boldsymbol{\theta}}^{ij} + \boldsymbol{\Pi}^{ij}\right)\ . \end{aligned} \tag{21}$$

The symmetric expression is obtained due to (16).

- *Homogenized shear elasticity* $\boldsymbol{\mathcal{G}} = (\mathcal{G}_{kl})$ introduced as

$$\begin{aligned} \mathcal{G}_{kl} &= \int_{Y_m} \gamma^m \partial_l^y (\tilde{w}^k + y_k) \\ &= \int_{Y_m} \gamma^m \nabla_y (\tilde{w}^k + y_k) \cdot \nabla_y (\tilde{w}^l + y_l) \ . \end{aligned} \tag{22}$$

The symmetric expression is obtained due to (17).

Inertia of the homogenized plate is represented by the following two mass coefficients:

$$\begin{aligned} \boldsymbol{\mathcal{M}}(\omega^2) &= \boldsymbol{I} \fint_Y \rho - \sum_r \frac{\omega^2}{\omega^2 - \lambda^r} \fint_{Y_c} \rho \boldsymbol{\Theta}^r \otimes \fint_{Y_c} \rho \boldsymbol{\Theta}^r \ , \\ \mathcal{N}(\omega^2) &= \fint_Y \rho - \sum_r \frac{\omega^2}{\omega^2 - \mu^r} \left| \fint_{Y_c} \rho W^r \right|^2 \ , \end{aligned} \tag{23}$$

see [1, 7] for derivation of the analogical mass coefficients in 3D elasticity problems. Influence of the load is weighted by the load coefficients which are computed by similar formulae

$$\begin{aligned} \boldsymbol{\mathcal{R}}(\omega^2) &= \boldsymbol{I} - \sum_r \frac{\omega^2}{\omega^2 - \lambda^r} \fint_{Y_c} \rho \boldsymbol{\Theta}^r \otimes \fint_{Y_c} \boldsymbol{\Theta}^r \ , \\ \mathcal{S}(\omega^2) &= 1 - \sum_r \frac{\omega^2}{\omega^2 - \mu^r} \fint_{Y_c} \rho W^r \fint_{Y_c} W^r \ . \end{aligned} \tag{24}$$

As the result of our homogenization procedure, we obtain Problem (14) where $(w, \boldsymbol{\theta})$ are the local amplitudes of harmonic waves excited by harmonic "homogenized" loads with frequency ω. Let us note that, when for some ω the tensor $\boldsymbol{\mathcal{M}}(\omega)$ is positive definite and the scalar $\mathcal{N}(\omega)$ is positive, then also free structure vibrations (i.e. stationary waves in domain Ω) can be excited. However, $\boldsymbol{\mathcal{M}}(\omega)$ or $\mathcal{N}(\omega)$ may not be positive (definite) for some ω; for the "membrane mode", cf. [1] and [7], we proved existence of whole frequency intervals – *the band gaps* – where the positiveness of $\boldsymbol{\mathcal{M}}(\omega)$ fails. An analogical result can be proved for the coupled rotational and deflection modes: in each interval of frequencies $\omega^2 \in (\lambda^r, \lambda^{r+1})$ given by (18) there exists a sub-interval of frequencies for which $\boldsymbol{\mathcal{M}}(\omega)$ is not positive. In such intervals, free vibration "rotation modes" may be restricted, or completely suppressed. Also for the shear modes associated with the deflection w and the corresponding mass $\mathcal{N}(\omega) < 0$, in each interval of frequencies $\omega^2 \in (\mu^r, \mu^{r+1})$ there may exist subintervals with restricted or suppressed wave propagation.

We show that for the coupled modes $\boldsymbol{q} := (\boldsymbol{\theta}, w)$ in plates, the dispersion analysis is more complex than in the 3D continuum. In Section 4.3, we discuss the band gap distribution using a numerical example. Interesting applications can be found [8].

Numerical illustration. To illustrate numerical modelling of the homogenized Reissner-Mindlin plate, in Fig. 1 we depict a finite element (FEM) approximation of corrector basis functions $\tilde{\boldsymbol{\theta}}^{rs}$ and $\tilde{w}^k$, see (16) and (17), as computed for a periodic structure made of cylindrical soft inclusions in a harder matrix. The material coefficients related to the microstructure are introduced in Table 1, the plate thickness is $h = 1$mm.

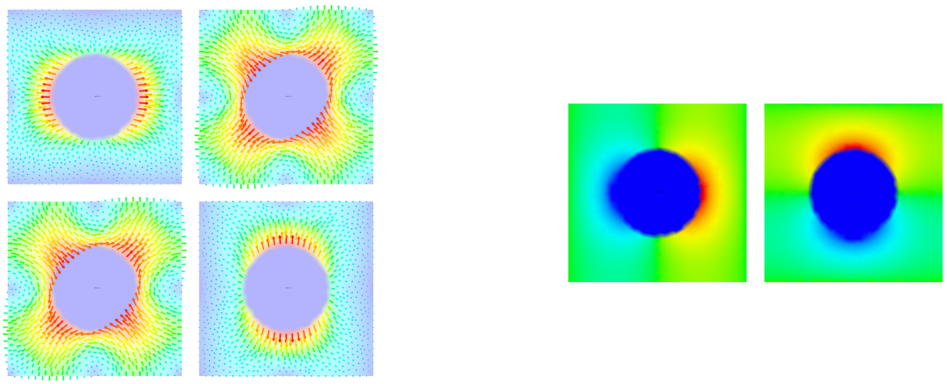

$\tilde{\boldsymbol{\theta}}^{rs}$ $\qquad\qquad$ $\tilde{w}^k$

Figure 1: Corrector basis function for the Reissner-Mindlin plate. Note: both $\tilde{\boldsymbol{\theta}}^{rs}$ and $\tilde{w}^k$, $r, s, k = 1, 2$ are computed just in the matrix part Y_m whereby Y_c is void. In the left figure, $\tilde{\boldsymbol{\theta}}^{rs}$ is represented by arrows, its magnitude $|\tilde{\boldsymbol{\theta}}^{rs}|$ by colors.

The homogenized mass coefficients are evaluated, for a given frequency ω, using the eigenmodes $(\boldsymbol{\Theta}^r, \lambda^r)$ and (W^r, μ^r), $r = 1, 2, \ldots$; the eigenfunctions are displayed in Fig. 2 for the first 12 modes computed on the cylindrical inclusion. The properties of matrix $\boldsymbol{\mathcal{M}}(\omega)$ and coefficient $\mathcal{N}(\omega)$ computed for this microstructure are discussed in Section 4.3.

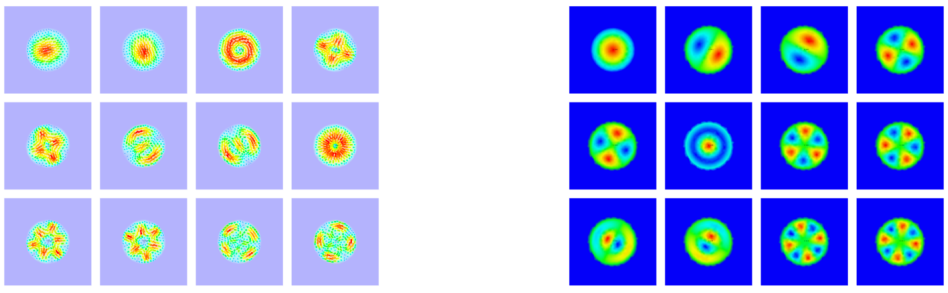

$|\boldsymbol{\Theta}^r|$ in Y_c $\qquad\qquad$ W^r in Y_c

Figure 2: Eigenmodes for the Reissner-Mindlin plate.

material par.	units:	in matrix Ω_m:	in inclusions Ω_c:
$(\lambda_{\mathbb{C}}, \mu_{\mathbb{C}})$	GPa	(50.898, 20.681)	(1.798, 1.483)
γ	GPa	10.0	0.5
ρ	10^3 kg/m^3	2.799	1.142

Table 1: Material parameters of the microscopic constituents. By $\lambda_{\mathbb{C}}, \mu_{\mathbb{C}}$ we denote the two Lamé stiffness coefficients.

3.3 Kirchhoff-Love phononic plate

In analogy with the Reissner-Mindlin plate model (13), we consider the elastic standing waves, cf. [5] for the plate homogenization. We find solutions to the following problem with the oscillating material coefficients: For a given frequency, find deflection $w^\varepsilon \in H^2_0(\Omega)$ such that

$$-\omega^2 h \int_{\Omega^\varepsilon_c} \rho^c w^\varepsilon v - \omega^2 h \int_{\Omega^\varepsilon_m} \rho^m w^\varepsilon v - \omega^2 \frac{h^3}{3} \int_{\Omega^\varepsilon_m} \rho^m \nabla w^\varepsilon \cdot \nabla v - \omega^2 \frac{h^3}{3} \int_{\Omega^\varepsilon_c} \rho^c \nabla w^\varepsilon \cdot \nabla v + \frac{h^3}{3} \int_{\Omega^\varepsilon_m} \mathbb{C}^m \nabla\nabla w^\varepsilon : \nabla\nabla v + \varepsilon^2 \frac{h^3}{3} \int_{\Omega^\varepsilon_c} \mathbb{C}^c \nabla\nabla w^\varepsilon : \nabla\nabla v = \int_\Omega (f v + \boldsymbol{m} \cdot \nabla v) \qquad \forall v \in H^2_0(\Omega)\ . \tag{25}$$

To present the homogenization result for $\varepsilon \to 0$, we proceed in analogy with the case of the Reissner-Mindlin plates. Using the unfolding method of homogenization [4] and obtain the following equation for the transversal deflections $w \in H^2_0(\Omega)$ such that

$$-\omega^2 h \int_\Omega \bar\rho w v - \omega^2 \frac{h^3}{3} \int_\Omega (\boldsymbol{\mathcal{M}}(\omega^2)\nabla w) \cdot \nabla v + \frac{h^3}{3} \int_\Omega (\boldsymbol{\mathcal{D}} \nabla\nabla w) : \nabla\nabla v = \int_\Omega \big([\boldsymbol{R}(\omega^2)\boldsymbol{m}] \cdot \nabla v + f v \big) \quad \forall v \in H^2_0(\Omega)\ , \tag{26}$$

where $\bar\rho$ is the average density of both material components situated in Y. Above $\boldsymbol{\mathcal{D}}$ is the 4th order homogenized bending stiffness tensor defined below in (31) and $\boldsymbol{\mathcal{M}}(\omega^2)$ is the homogenized mass tensor computed using a similar expression to (23), see (32). The "effective material parameters" are defined in terms of the characteristic microscopic responses.

Characteristic microscopic responses. In contrast with the Reissner-Mindlin plates, the cross-section rotations in the Kirchhoff-Love theory are fully determined by the gradients of deflections; consequently only two instead of four microscopic problems must be solved. The corrector basis function $\tilde w^{kl} \in H^2_\#(Y_m)$ solves the following

equation

$$\int_{Y_m} \left[\mathbb{C}^m \nabla\nabla_{yy}(\tilde{w}^{kl} + \Pi^{kl})\right] : \nabla\nabla_{yy}\tilde{v} = 0 \quad \forall \tilde{v} \in H^2_{\#}(Y) \ , \tag{27}$$

where $\Pi^{kl} = y_k y_l$. To compute the homogenized mass tensor, one needs to solve the local problem: find $(\lambda^r, \boldsymbol{\varphi}^r) \in \mathbb{R} \times \boldsymbol{W}(Y_c)$ satisfying

$$\int_{Y_c} [\mathbb{C}^c \nabla_y \boldsymbol{\varphi}^r] : \nabla_y \boldsymbol{\vartheta} = \lambda^r \int_{Y_c} \rho \boldsymbol{\varphi}^r \cdot \boldsymbol{\vartheta} \qquad \forall \boldsymbol{\vartheta} \in \boldsymbol{W}(Y_c) \ , \tag{28}$$

where we employ the spaces of rotation-free vector fields:

$$\boldsymbol{W}(Y_c) = \{\boldsymbol{w} \in \mathbf{H}^1_{\#}(Y_c) |\ \nabla_y \times \boldsymbol{w} = 0\} \ . \tag{29}$$

Obviously, due to the ellipticity of the operator in (28), functions $\{\boldsymbol{\varphi}^r\}_r$ form an orthogonal system; we use the standard normalization

$$\int_{Y_c} \rho \boldsymbol{\varphi}^r \cdot \boldsymbol{\varphi}^s = \delta_{rs} \ . \tag{30}$$

Homogenized coefficients. The homogenized Kirchhoff-Love plate model involves the following material coefficients defined in terms of the characteristic responses just introduced:

- *Homogenized elastic coefficients* $\boldsymbol{\mathcal{D}} = (\mathcal{D}_{ijkl})$

$$\begin{aligned} \mathcal{D}_{ijkl} =& \fint_{Y_m} [\mathbb{C}^m \nabla\nabla_{yy}(\tilde{w}^{kl} + \Pi^{kl})] : \nabla\nabla_{yy}\Pi^{ij} \\ =& \fint_{Y_m} [\mathbb{C}^m \nabla\nabla_{yy}(\tilde{w}^{kl} + \Pi^{kl})] : \nabla\nabla_{yy}(\pi^{ij} + \Pi^{ij}) \ , \end{aligned} \tag{31}$$

  where the symmetric expression follows due to (27);

- *Homogenized mass tensor* $\boldsymbol{\mathcal{M}} = (\mathcal{M}_{ij})$

$$\boldsymbol{\mathcal{M}}(\omega^2) = \boldsymbol{I} \fint_Y \rho - \sum_{r \geq 1} \frac{\omega^2}{\omega^2 - \lambda^r} \fint_{Y_c} \rho \boldsymbol{\varphi}^r \otimes \fint_{Y_c} \rho \boldsymbol{\varphi}^r \ . \tag{32}$$

- *Homogenized load coefficient* $\boldsymbol{\mathcal{R}} = (\mathcal{R}_{ij})$

$$\boldsymbol{\mathcal{R}}(\omega^2) = \boldsymbol{I} - \sum_{r \geq 1} \frac{\omega^2}{\omega^2 - \lambda^r} \fint_{Y_c} \rho \boldsymbol{\varphi}^r \otimes \fint_{Y_c} \boldsymbol{\varphi}^r \ . \tag{33}$$

By virtue of the right-hand side expression in (32), $\boldsymbol{\mathcal{M}}(\omega^2)$ can be negative, or negative semi-definite for some frequencies ω. In such a case, standing wave propagation could be restricted or even suppressed for modes characterized by the deflection gradient $\boldsymbol{\psi} := \nabla w$ being the eigenvector associated with the non-positive eigenvalue of $\boldsymbol{\mathcal{M}}(\omega^2)$. However, the theory explained in [1] for the standard 3D elasticity cannot be simply adopted, because the first left hand side term in (26) does not change its sign and contributes to the positive inertia even for negative $\boldsymbol{\mathcal{M}}(\omega^2)$.

4 Dispersion analysis

We consider guided waves in the homogenized plates. In what follows we employ plane waves of the frequency ω propagating in the direction $\boldsymbol{n}$, whereby the wave length is given by the wave number $\varkappa$. Let $\bar{\boldsymbol{\theta}}$ and $\bar{w}$ be the amplitudes, then

$$\begin{aligned} \boldsymbol{\theta}(x) &= \bar{\boldsymbol{\theta}} e^{\mathrm{i}\varkappa \boldsymbol{n}\cdot\boldsymbol{x}} \ , \\ w(x) &= \bar{w} e^{\mathrm{i}\varkappa \boldsymbol{n}\cdot\boldsymbol{x}} \ . \end{aligned} \tag{34}$$

4.1 Reissner-Mindlin plates

The wave equation of the homogenized plate is obtained from (14)

$$\begin{aligned} -\frac{h^3}{3}\nabla\cdot\mathbb{D}\boldsymbol{e}(\boldsymbol{\theta}) - h\boldsymbol{\mathcal{G}}(\nabla w - \boldsymbol{\theta}) &= \omega^2 \frac{h^3}{3}\boldsymbol{\mathcal{M}}(\omega^2)\boldsymbol{\theta} \ , \\ -h\nabla\cdot\boldsymbol{\mathcal{G}}(\nabla w - \boldsymbol{\theta}) &= \omega^2 h\mathcal{N}(\omega^2) w \ , \end{aligned} \tag{35}$$

We shall employ the following notation:

$$\boldsymbol{\mathcal{A}} = \mathbb{D} : (\boldsymbol{n}\otimes\boldsymbol{n}) \ , \quad \boldsymbol{b} = \boldsymbol{\mathcal{G}}\boldsymbol{n} \ , \quad g = \boldsymbol{\mathcal{G}} : (\boldsymbol{n}\otimes\boldsymbol{n}) \ . \tag{36}$$

On substituting the wave ansatz (34) in (35), we get the dispersion equation:

$$\begin{pmatrix} \varkappa^2 \frac{h^3}{3}\boldsymbol{\mathcal{A}} + h\boldsymbol{\mathcal{G}}, & -\mathrm{i}\varkappa h\boldsymbol{b} \\ \mathrm{i}\varkappa h\boldsymbol{b}\cdot, & \varkappa^2 h g \end{pmatrix} \begin{pmatrix} \bar{\boldsymbol{\theta}} \\ \bar{w} \end{pmatrix} = \omega^2 \begin{pmatrix} \frac{h^3}{3}\boldsymbol{\mathcal{M}}(\omega^2), & 0 \\ 0, & h\mathcal{N}(\omega^2) \end{pmatrix} \begin{pmatrix} \bar{\boldsymbol{\theta}} \\ \bar{w} \end{pmatrix} \ . \tag{37}$$

We can now discus computing the wave numbers and distinguish some special modes.

First, let us assume $\omega^2\mathcal{N}(\omega^2) - \varkappa^2 g \neq 0$, then $\bar{w}$ can be eliminated from (37) using

$$\bar{w} = \frac{\mathrm{i}\varkappa \boldsymbol{b}\cdot\bar{\boldsymbol{\theta}}}{\omega^2\mathcal{N}(\omega^2) - \varkappa^2 g} \ , \tag{38}$$

therefore, there is a $\pi/2$ phase shift between the rotation and deflection amplitudes. Consequently (37) can be rewritten, as follows:

$$\varkappa^2 \left(\frac{h^3}{3}\boldsymbol{\mathcal{A}} + h(\omega^2\mathcal{N}(\omega^2) - \varkappa^2 g)^{-1}\boldsymbol{b}\otimes\boldsymbol{b} \right) \bar{\boldsymbol{\theta}} = \left(\omega^2 \frac{h^3}{3}\boldsymbol{\mathcal{M}}(\omega^2) - h\boldsymbol{\mathcal{G}} \right) \bar{\boldsymbol{\theta}} \ . \tag{39}$$

Thus, we obtain the following biquadratic equation to be solved for $(\varkappa, \bar{\boldsymbol{\theta}})$:

$$\left(\varkappa^4 \boldsymbol{R} - \varkappa^2 \boldsymbol{S}(\omega) + \boldsymbol{T}(\omega) \right) \bar{\boldsymbol{\theta}} = 0 \ , \tag{40}$$

where

$$\begin{aligned}
\boldsymbol{R} &= g\frac{h^2}{3}\boldsymbol{\mathcal{A}}\,,\\
\boldsymbol{S}(\omega) &= \omega^2\frac{h^2}{3}\left(\mathcal{N}(\omega^2)\boldsymbol{\mathcal{A}} + g\boldsymbol{\mathcal{M}}(\omega^2)\right) + \boldsymbol{b}\otimes\boldsymbol{b} - g\boldsymbol{\mathcal{G}}\,,\\
\boldsymbol{T}(\omega) &= \omega^2\mathcal{N}(\omega^2)\left(\omega^2\frac{h^2}{3}\boldsymbol{\mathcal{M}}(\omega^2) - \boldsymbol{\mathcal{G}}\right)\,.
\end{aligned} \tag{41}$$

Eq. (40) can be rewritten using substitution $\bar{\psi} = -\varkappa^2\mathbf{L}^T\bar{\boldsymbol{\theta}}$ with $\mathbf{L}\mathbf{L}^T = \boldsymbol{R}$ (note $\boldsymbol{\mathcal{A}}$ is symmetric pos. def.), so that $\varkappa^2$ can be computed by solving the following eigenvalue problem:

$$\begin{pmatrix} \boldsymbol{S}(\omega), & \mathbf{L} \\ \mathbf{L}^T, & 0 \end{pmatrix}\begin{pmatrix} \bar{\boldsymbol{\theta}} \\ \bar{\psi} \end{pmatrix} = \frac{1}{\varkappa^2}\begin{pmatrix} \boldsymbol{T}(\omega), & 0 \\ 0, & -\boldsymbol{I} \end{pmatrix}\begin{pmatrix} \bar{\boldsymbol{\theta}} \\ \bar{\psi} \end{pmatrix}\,. \tag{42}$$

Obviously, if both $\boldsymbol{S}(\omega^2)$ and $\boldsymbol{T}(\omega^2)$ are positive definite (both are symmetric), whereby the left-hand side matrix is also positive definite, then $\varkappa^2 > 0$, so that there are two guided waves. Otherwise *band gaps* can occur; we shall demonstrate such situations in the next Section.

Let us recall that (42) is eligible for $\omega^2\mathcal{N}(\omega^2) \neq \varkappa^2 g$. In the opposite case, we get formally $\varkappa^2\boldsymbol{S}(\omega) - \boldsymbol{T}(\omega) = \varkappa^2\left(\omega^2\frac{h^3}{3}\mathcal{N}(\omega^2)\boldsymbol{\mathcal{A}} + h^2\boldsymbol{b}\otimes\boldsymbol{b}\right)$. Consequently, (40) reads as $\varkappa^2\boldsymbol{b}\otimes\boldsymbol{b}\bar{\boldsymbol{\theta}} = 0$, thus, $\boldsymbol{b}\perp\bar{\boldsymbol{\theta}}$. Clearly, in this case we recover the mode which will be just described.

Special modes with $\boldsymbol{b}\perp\bar{\boldsymbol{\theta}}$. Let us now assume $\omega^2\mathcal{N}(\omega^2) = \varkappa^2 g$, thus, (38) is invalid. On denoting $\boldsymbol{\mathcal{B}}(\omega^2) = \omega^2\frac{h^3}{3}\boldsymbol{\mathcal{M}}(\omega^2) - h\boldsymbol{\mathcal{G}}$, from (37) we deduce the following eigenvalue problem

$$\begin{aligned}
\boldsymbol{\mathcal{B}}(\omega^2)\bar{\boldsymbol{\theta}} + \boldsymbol{b}\eta &= \varkappa^2\frac{h^3}{3}\boldsymbol{\mathcal{A}}\bar{\boldsymbol{\theta}}\,,\\
\boldsymbol{b}\cdot\bar{\boldsymbol{\theta}} &= 0\,,
\end{aligned} \tag{43}$$

where $\eta = \bar{w}$ is the Lagrange multiplier of constraint $\boldsymbol{b}\perp\bar{\boldsymbol{\theta}}$. Recalling $\omega^2\mathcal{N}(\omega^2) = \varkappa^2 g$, due to the comparison between (43) and (37) we can observe that $\bar{w} = \eta$.

However, assuming $\omega^2\mathcal{N}(\omega^2) \neq \varkappa^2 g$, when $\boldsymbol{b}\cdot\bar{\boldsymbol{\theta}} = 0$, deflections vanish, i.e. $\bar{w} = 0$, by virtue of (38). In this case, (39) reduces to (43) where $\eta = 0$. A nontrivial *"hour-glass" rotational mode* must satisfy

$$\bar{\boldsymbol{\theta}} \in \ker\left(\boldsymbol{\mathcal{B}}(\omega^2) - \varkappa^2\frac{h^3}{3}\boldsymbol{\mathcal{A}}\right)\cap\ker\boldsymbol{b}^T\,. \tag{44}$$

Condition (44) can be reformulated, as follows: take $\hat{\boldsymbol{\theta}} = \boldsymbol{b}^\perp$ with $|\hat{\boldsymbol{\theta}}| = 1$, and express $\boldsymbol{f}(\omega^2,\varkappa^2) := (\boldsymbol{\mathcal{B}}(\omega^2) - \varkappa^2\frac{h^3}{3}\boldsymbol{\mathcal{A}})\hat{\boldsymbol{\theta}}$. Now (44) holds for $\hat{\boldsymbol{\theta}}$ whenever $\boldsymbol{f}(\omega^2,\varkappa^2) = 0$, which presents a system of two equations for $(\omega^2,\varkappa^2)$. Obviously, only real positive solutions possess a wave mode.

4.2 Kirchhoff-Love plates

We follow a similar procedure like the one performed in analysis of waves in the Reissner-Mindlin plates. For any plane wave given in (34), the Kirchhoff-Love plate equation (with zero external loads, assuming fully clamped plate)

$$-\omega^2 h\bar{\rho}w + \omega^2\frac{h^3}{3}\nabla\cdot\boldsymbol{\mathcal{M}}(\omega^2)\nabla w + \frac{h^3}{3}\nabla\nabla : (\boldsymbol{\mathcal{D}}\nabla\nabla w) = 0 \tag{45}$$

takes the following form:

$$-\omega^2 h\bar{\rho}\bar{w} - \omega^2\varkappa^2\frac{h^3}{3}\boldsymbol{\mathcal{M}}(\omega^2) : \boldsymbol{n}\otimes\boldsymbol{n}\bar{w} + \varkappa^4\frac{h^3}{3}\boldsymbol{n}\otimes\boldsymbol{n} : \boldsymbol{\mathcal{D}}(\boldsymbol{n}\otimes\boldsymbol{n})\bar{w} = 0\ . \tag{46}$$

Denoting

$$\hat{d} = \boldsymbol{n}\otimes\boldsymbol{n} : \boldsymbol{\mathcal{D}}(\boldsymbol{n}\otimes\boldsymbol{n})\ , \quad \text{and} \quad \hat{m}(\omega^2) = \boldsymbol{\mathcal{M}}(\omega^2) : \boldsymbol{n}\otimes\boldsymbol{n}\ , \tag{47}$$

(46) yields a biquadratic equation for wave numbers $\varkappa$ of plane waves propagating in direction $\boldsymbol{n}$,

$$\varkappa^4\hat{d} - \varkappa^2\omega^2\hat{m}(\omega^2) - \omega^2\frac{3\bar{\rho}}{h^2} = 0\ . \tag{48}$$

It is worth noting that if no inertia related to cross-section rotations was considered, i.e. $\hat{m}\equiv 0$ *a priori*, the dispersion relation (48) would possess $\varkappa^2 = \pm\omega/h\sqrt{3\bar{\rho}/\hat{d}}$. However, in our case with mass $\boldsymbol{\mathcal{M}}(\omega^2)$ related to the rotations the dispersion formula yields the following expression for $\vartheta = \varkappa^2/\omega^2$ where

$$\vartheta_{\pm} = \frac{\hat{m}(\omega^2) \pm \sqrt{\left(\hat{m}(\omega^2)\right)^2 + 12\frac{\bar{\rho}\hat{d}}{h^2\omega^2}}}{2\hat{d}}\ . \tag{49}$$

This relation reveals that a propagating wave exists for any frequency ω. Indeed, even for $\boldsymbol{\mathcal{M}}(\omega^2)$ negative (semi)definite, such that $\hat{m}(\omega^2) < 0$, we have always $\vartheta_+ > 0$ independently of ω. Thus, in contrast with the Reissner-Mindlin plates, the homogenized Kirchhoff-Love model *does not admit band gaps* for guided waves.

4.3 Computing band gaps for the Reissner-Mindlin phononic plates

In this section we use the same plate microstructure generated by cylindrical inclusions, with material properties listed in Table 1, for which some illustrations of computed corrector basis functions and eigenmodes were introduced. The aim of this section is to show some interplay between eigenmodes of the inclusion and the band gaps identified from the dispersion analysis. It performs in the following steps (see [7] for the analogical procedure of computing the dispersion curves in a 3D phononic homogenized composite):

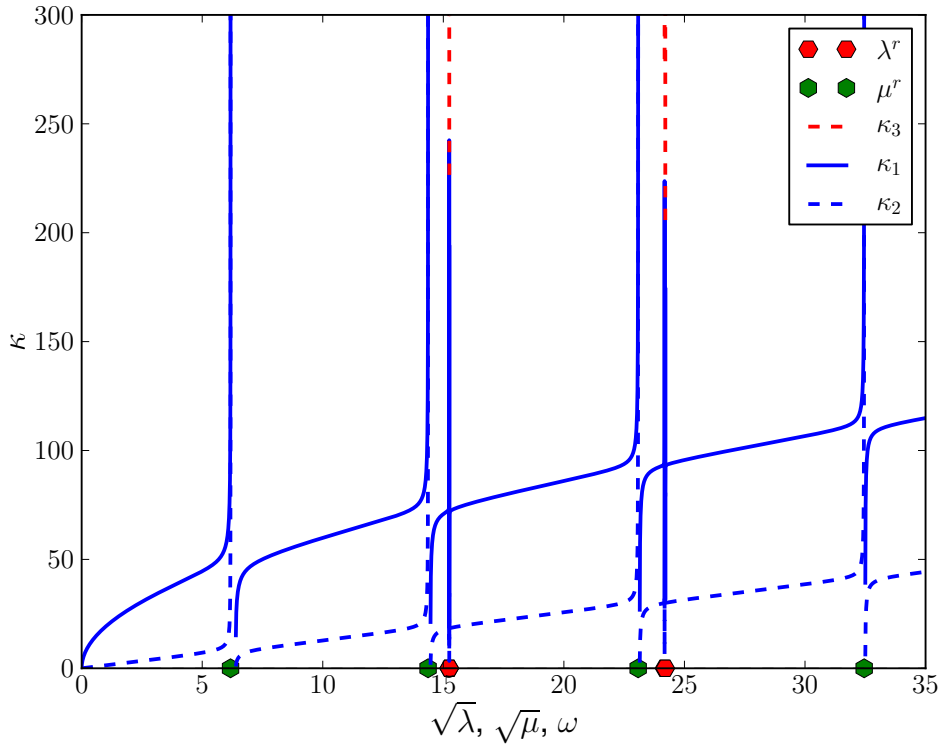

Figure 3: Dispersion curves of two modes for the Reissner-Mindlin plate. There is at least one small band gap $[6.174, 6.392]$Hz, while 3 others have almost negligible lengths. The resonance frequencies of the vibration modes in the elastic inclusions are marked by points on the frequency axis, see Table 2.

1. Compute the microscopic response, i.e., the corrector rotations $\tilde{\theta}^{rs}$ and deflections $\tilde{w}^k$, and the eigenmodes $(\boldsymbol{\Theta}^r, \lambda^r)$ and (W^r, μ^r), $r = 1, 2, \ldots$.

2. Compute homogenized coefficients $\mathcal{D}$, $\mathcal{G}$.

3. For a given direction of wave propagation and any given frequency $\omega \in [\underline{\omega}, \overline{\omega}]$:

   (a) compute homogenized masses $\boldsymbol{\mathcal{M}}(\omega)$ and $\mathcal{N}(\omega)$,

   (b) constitute matrices $\boldsymbol{R}, \boldsymbol{S}(\omega), \boldsymbol{T}(\omega)$,

   (c) solve the generalized eigenvalue problem (42) to obtain $(\bar{\boldsymbol{\theta}}^k, \bar{\boldsymbol{\psi}}^k)$ and $\Lambda^k := 1/\varkappa^k$, $k = 1, 2, 3, 4$. It should be noted that complex eigennumbers Λ^k are obtained when the left-hand side matrix involving $\boldsymbol{S}(\omega)$, or matrix $\boldsymbol{T}(\omega)$ are not both positive definite.

   (d) Select only real positive $\Lambda^{\hat{k}}$, $\hat{k} \in \{1, 2, 3, 4\}$, such that $\varkappa^{\hat{k}} := 1/\sqrt{\Lambda^{\hat{k}}}$ is the wave number of a propagating wave, i.e. $(\omega, \varkappa^{\hat{k}})$ is one point of a dispersion curve.

4. Display the point-wise computed curves, see Fig. 3.

Using this algorithm we analyzed band gaps in the frequency range 0 to 35 Hz. In Fig. 3 two wave modes $\varkappa_1$ and $\varkappa_2$ are represented by dispersion curves, whereby the gaps can be observed in intervals (ω^-, ω^+) identified by unbounded slopes of the $\varkappa(\omega)$ functions, i.e. $\lim_{\omega \to \omega^-} \varkappa(\omega) = +\infty$ and $\lim_{\omega \searrow \omega^+} \varkappa(\omega) = -\infty$. In contrast with the 3D phononic structure, see [7], where the band gaps can be directly analyzed using eigenvalues of the mass tensor, [1], apparently for plates analogical conclusions cannot be deduced, as can be seen by comparing Fig. 3 with illustrations of eigenvalues of $\boldsymbol{\mathcal{M}}(\omega)$ and values of $\mathcal{N}(\omega)$, see Fig. 4 and Fig. 5.

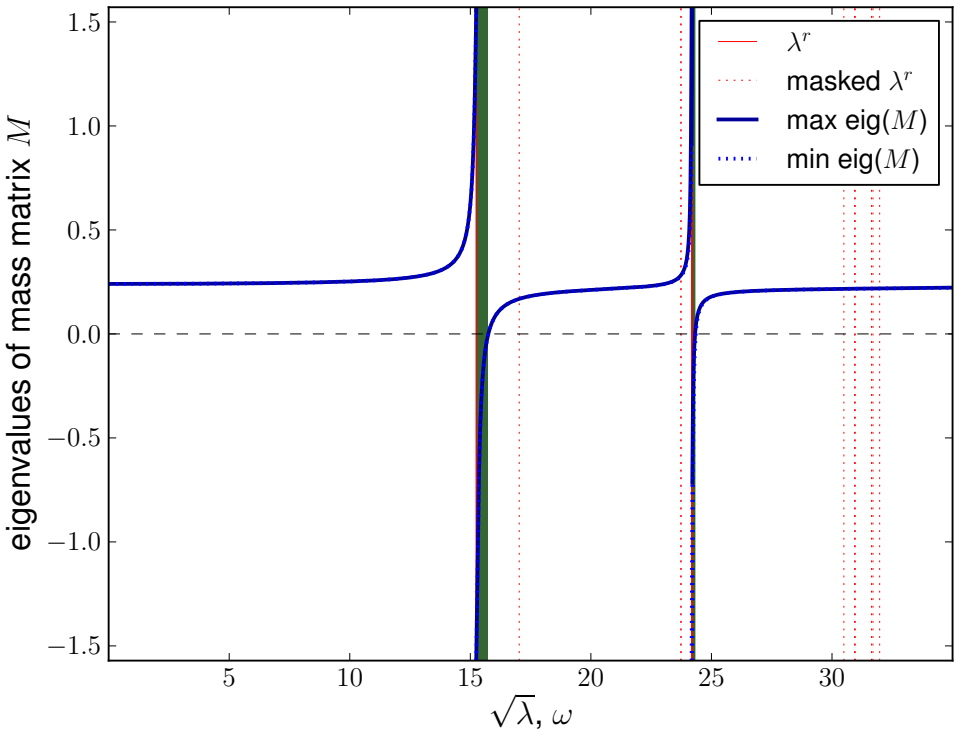

Figure 4: The eigenvalues of the mass matrix $\boldsymbol{\mathcal{M}}(\omega^2)$. There are two intervals where both eigenvalues are negative.

mode:	μ^1	μ^1	λ^1	λ^2	μ^3	λ^3	λ^4	μ^4
Hz	6.175	14.368	15.245	15.247	23.080	24.177	24.206	32.458

Table 2: Resonance frequencies < 35 Hz with nonzero mean of the associated eigenfunctions (see formulae (23)) for the eigenvalue problems (18) and (19). Note: $\lambda^1 \approx \lambda^2$ and $\lambda^3 \approx \lambda^4$ should be double frequencies due to the structure symmetry.

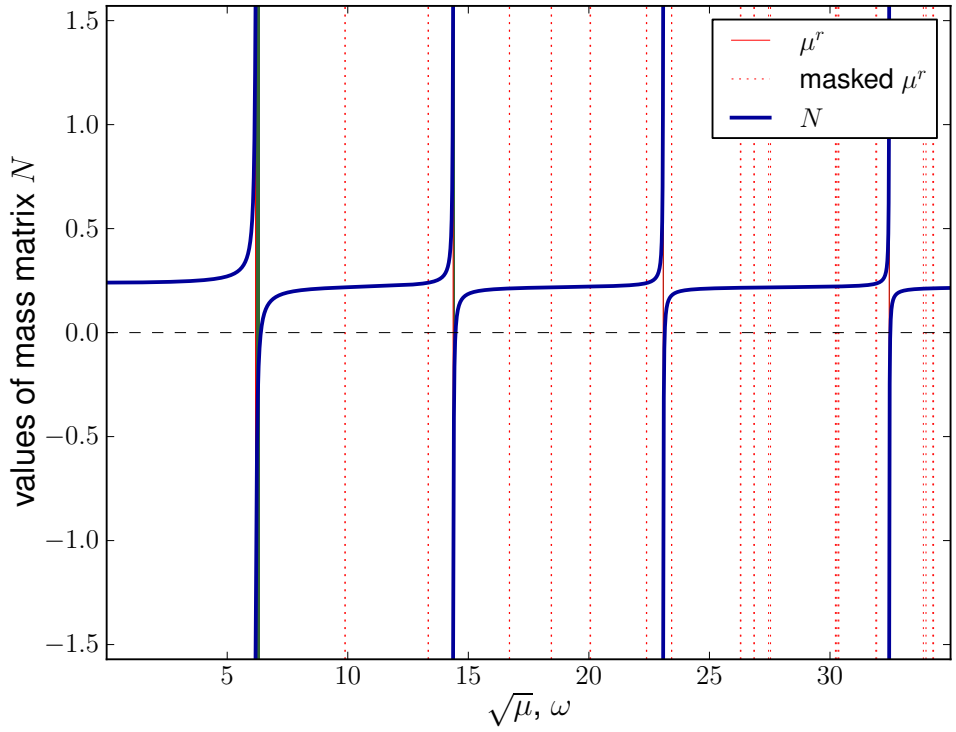

Figure 5: Values of $\mathcal{N}(\omega)$ can be negative, as observed in 4 small intervals.

5 Conclusions

We presented homogenized models of wave propagation in strongly heterogeneous plates, considering the Reissner-Mindlin (R-M) and the Kirchhoff-Love (K-L) theories; while the first one takes into account shear effects related to rotations of the plate cross-section with respect to the mid-plane, the second theory neglects this phenomenon, which makes it convenient rather for thin plates. The homogenization results reveal dispersion properties for the homogenized plates: we conjecture, with reference to the 3D phononic crystals, that there exist bands of frequencies for which the wave equations admit evanescent solutions only, at least for certain polarizations. There is a remarkable difference between the R-M and K-L models: while for R-M the wave polarization is determined by components of $(\boldsymbol{\theta}, w)$, i.e. the rotation and deflection, for K-L there is just a scalar wave associated with the deflection w.

An important restriction of both presented models is related to the transversal isotropy: here only cylindrical inclusions are admissible, although their shapes can be arbitrary. To treat more general composite plates with e.g. spheroidal inclusions, the homogenization procedure must be applied to a 3D composite with thickness proportional to ε, i.e. to the microstructure scale.

The phononic effect, in general, is associated with vibration modes excited at the

"microscopic" level. By virtue of definitions (23) and (32), these modes determine "positivity", or "negativity" of the homogenized masses; in [1] we described how this observation can be employed to predict band gaps in the 3D phononic crystals. The classical method of the band gap identification is based on analysis of guided waves, thus, upon construction of dispersion curves; it is necessary to compute frequencies for selected wave numbers ranging the Brillouin zone, cf. [7]. Although a detailed study of the band gaps for the presented models is an issue of our further research, using a numerical example we demonstrated existence of band gaps in a guided wave propagation in an infinite homogenized R-M plate. For the K-L plate a simple calculation shows that there is always a propagating wave even if the mass tensor associated with the plate rotations is negative definite. For standing waves the band gap phenomenon will be studied separately, as in that case the influence of boundary conditions must be respected.

Acknowledgments

The research of E.R. was supported by the European Regional Development Fund (ERDF), project "NTIS – New Technologies for Information Society", European Centre of Excellence, CZ.1.05/1.1.00/02.0090, and in part by the Czech Scientific Foundation project GACR P101/12/2315.

References

[1] A. Ávila, G. Griso, B. Miara, and E. Rohan. Multiscale modeling of elastic waves: Theoretical justification and numerical simulation of band gaps. *Multiscale Modeling & Simulation, SIAM*, 7:1–21, 2008.

[2] R. Cimrman and E. Rohan. Three-phase phononic materials. *Appl. Comp. Mech.*, 3:5–16, 2009.

[3] R. Cimrman and E. Rohan. On acoustic band gaps in homogenized piezoelectric phononic materials. *Appl. Comp. Mech.*, 4:89–100, 2010.

[4] D. Cioranescu, A. Damlamian, and G. Griso. The periodic unfolding method in homogenization. *SIAM Journal on Mathematical Analysis*, 40(4):1585–1620, 2008.

[5] M. Ghergu, G. Griso, H. Mechkour, and B. Miara. Homogenization of thin perforated plates. *ESAIM: Mathematical Modelling and Numerical Analysis*, 56:875–895, 2007.

[6] E. Rohan and B. Miara. Band gaps and vibration of strongly heterogeneous reissner-mindlin elastic plates. *Comptes Rendus Mathematique*, 349:777–781, 2011.

[7] E. Rohan, B. Miara, and F. Seifrt. Numerical simulation of acoustic band gaps in homogenized elastic composites. *International Journal of Engineering Science*, 47:573—-594, 2009.

[8] J.O. Vasseur, P.A. Deymier, B. Djafari-Rouhani, and Y. Pennec. Absolute forbidden bands and waveguiding in two-dimensional phononic crystal plates. *Phys. Rev. B*, 77, 2008.